Journal of Quality Measurement and Analysis *JQMA* 22(2) 2026, 329-346
e-ISSN: 2600-8602 *http://www.ukm.my/jqma*
https://doi.org/10.17576/jqma.2202.2026.18

COMPARATIVE ANALYSIS OF MATHEMATICAL MODELS FOR ESTIMATING DISCHARGE RATIO IN TRAPEZOIDAL CROSS-SECTION OPEN-CHANNEL DIVIDING FLOW

(*Analisis Perbandingan Model Matematik bagi Menganggar Nisbah Pelepasan dalam Aliran Pembahagi Saluran Terbuka Keratan Rentas Trapezoid*)

PUTERI NADIA SHAFIQAH HARMIZI, ISKANDAR SHAH MOHD ZAWAWI*, MOHD RIDZA MOHD HANIFFAH & SITI AIMI ASYARAH ZAKARIA

ABSTRACT

Dividing flow in open-channel is the phenomenon where a single channel splits into several smaller channels. It may also arise at junctions where two or more channels converge. Therefore, it is important to predict the behavior of the flow under certain conditions and makes estimation about the effect of changes in dividing angles on the flow behavior. This study deals with the development of the mathematical model of dividing flow for trapezoidal cross-sectional channel by considering the Reynold's number to estimate the discharge ratio at certain dividing angles. Model's performance is validated through the comparison of its predictive accuracy relative to the simulation results obtained by the computational fluid dynamics software. The findings demonstrate that the proposed model with Reynold's number produces better accuracy with lower deviation percentage compared to the existing model with Froude number. This suggests that the proposed model may be a viable alternative to more computationally intensive simulation software to estimate the discharge in the channel after junction and branch channel.

Keywords: discharge ratio; dividing flow; Reynold's number; mathematical modelling

ABSTRAK

Aliran terbahagi dalam saluran terbuka ialah fenomena di mana satu saluran tunggal terbahagi kepada beberapa saluran yang lebih kecil. Ia juga boleh berlaku di persimpangan di mana dua atau lebih saluran bertemu. Oleh itu, pemodelan matematik adalah penting untuk meramalkan tingkah laku aliran di bawah keadaan tertentu dan membuat anggaran tentang kesan perubahan sudut pembahagian terhadap tingkah laku aliran. Kajian ini memberi tumpuan kepada pembangunan model matematik bagi aliran terbahagi untuk saluran berkeratan rentas trapezoid dengan mengambil kira nombor Reynold untuk menganggarkan nisbah pelepasan pada sudut pembahagian tertentu. Prestasi model disahkan melalui perbandingan ketepatan ramalannya berbanding keputusan simulasi yang diperoleh daripada perisian dinamik bendalir pengkomputeran. Penemuan menunjukkan bahawa model yang dicadangkan dengan nombor Reynold menghasilkan ketepatan yang lebih baik dengan peratusan sisihan yang lebih rendah berbanding model sedia ada dengan nombor Froude. Ini menunjukkan bahawa model yang dicadangkan boleh menjadi alternatif yang berdaya maju kepada perisian simulasi yang memerlukan intensiti pengkomputeran yang tinggi untuk menganggar kadar alir dalam saluran selepas persimpangan dan saluran cawangan.

Kata kunci: nisbah discaj; aliran terbahagi; nombor Reynold; permodelan matematik

1. Introduction

Various forces acting on open-channel flow significantly affect its hydraulic behavior. Among these, the dimensionless Froude number is essential in analysing the effect of gravity in fluid flow and describes the flow behavior. It is technically defined as the square root of the ratio of inertial forces and gravitational forces (Karimi 2014). The value of Froude number determines three types of flow; critical, subcritical, and supercritical, which affect the behavior of the water surface and the occurrence of hydraulic jumps, a natural phenomenon that occurs specifically when the flow transition abruptly from supercritical to subcritical. A sub-critical flow or tranquil range of flow happens when the value of Froude number is less than one, in which gravity forces dominate and channel is deep, hence the flow moves slowly with a low energy state. If the inertial forces dominate where flow moves fast with a high energy state, then the channel is shallow and possesses the value of Froude number greater than one (Azimi & Shabanlou 2016). A critical flow happens when the Froude number is one, it means that the inertial forces and gravity are equivalent.

Reynold's number is a non-dimensional parameter which represents the effect of viscosity relative to inertia. The flow in the channel changes from laminar to turbulent if depending on the Reynold's number. The Froude number and Reynold's number are quite similar since both measure the energy state of flow depending on the velocity of the flow, which can be calculated by using Manning velocity equation. The Reynolds number considers the viscosity of water, whereas the Froude number is only concerned with the water's depth and does not consider viscosity. When the temperature of water increases, then the viscosity decreases (Ahammed *et al.* 2016; Esfe *et al.* 2016; Toghraie *et al.* 2016).

River bifurcations or diffluence are divisions in the flow and sediment transport from a single channel to several branches or distributaries that occur due to morphological processes (Ibrahim *et al.* 2020; Kleinhans *et al.* 2013). It is a significant measure recommended by authorities to mitigate rivers overflow during intense rainfall. To avoid any dreadful consequences such as corrosion that can drown the areas, the flow must be more evenly distributed uniformly to maintain its stability, which can benefit aquatic ecosystems and human activities (Liu & Li 2013). Therefore, the impact of varying branching channel geometries including bifurcation angles on flow distribution uniformity was studied by Cao *et al.* (2018). One of the conclusions made is such flow deteriorates with the increase of angles, while the worst performance occurs when angle is 90°. An experimental study of predicting sediment transport with diversion angles of 30°, 45°, 60°, 75° and 90° was made by Alomari *et al*. (2020). The experiment found that the sediment discharge is manageable by changing the diversion angle from 90° to 30° and 60°. Furthermore, Malik and Abdul Matin (2021) found that discharge ratio of branch to main channel increases as diversion angles of 20°, 40° and 60° increases. Previous works have considered the division angles below 90° (Alomari *et al.* 2016; Cao *et al.* 2018; Harmizi & Zawawi 2024; Pandey & Mishra 2012; Shahari *et al.* 2021).

Most of the previous studies that related to the open channel dividing flows are commonly encountered with engineering applications such as physical experiments and three-dimensional (3D) model simulations (Alfatlawi & Hussein 2024). Abu-Zaid (2023) applied the theoretical 3D ANSYS 16 software to investigate the diverted flow into bifurcating channels with different diversion angles (15°, 30°, 45°, 60°, 75° and 90°). The results proved that the 15° diversion angle yields the most optimum impact on the diverted flow in a rectangular-sectioned open-channel system.

Instead of constructing superfluous structures, experimental setups, and costly physical models, it is important to carry out the derivation of mathematical models that can be used in the hydraulic analysis and provide accurate results in engineering practice. Cheng *et al.* (2018) applied the theory of algebraic inequality to determine the critical depth of a steady non-uniform flow in open channel model. The mathematical models based on momentum principle and continuity equation were introduced by Pandey and Mishra (2012) to compare the flow depth features of combining and dividing flow. The general equation of dividing flow in a trapezoidal channel based on Froude number is given as follows (Pandey & Mishra 2012):

$$
\begin{aligned}
&(1+2k_1)\left\{\frac{1}{2}\left(y_r^2-1+y_r^2 Br_3\cos\theta_3\right)+\frac{k_1}{3}\left[y_r^2(1+\cos\theta_3)-1\right]\right\} \\
&=F_1^2(1+k_1)^2\left\{1-C\left[(1-q_r)\sin\theta_2+q_r\sin\theta_3\right]-\frac{(1+k_1)}{y_r}\left[\frac{(1-q_r)^2\cos\theta_2}{Br_2+k_1y_r}+\frac{q_r^2\cos\theta_3}{Br_3+k_1y_r}\right]\right\}. \qquad (1)
\end{aligned}
$$

Subscripts 2 and 3 represent the branches, while subscript 1 represents the main channel. The depth ratio is different in upstream and downstream, and this may be associated with the reason in which to prevent channel overflow. Then, Eq (1) was reconstructed by Zawawi *et al.* (2019) in which there is slightly different in terms of the power of three of flow depth ratio, y_r^3 as shown in the following equation:

$$
\begin{aligned}
&(1+2k_1)\left[\frac{1}{2}\left(1-y_r^2-Br_2y_r^2\cos\theta_2\right)+\frac{k_1}{3}\left(1-y_r^3-y_r^3\cos\theta_2\right)\right] \\
&=F_1^2(1+k_1)^2\left\{\frac{(1+k_1)}{y_r}\left[\frac{(1-q_r)^2}{Br_3+k_1y_r}\cos\theta_3+\frac{q_r^2}{Br_2+k_1y_r}\cos\theta_2\right]-1+C\left[(1-q_r)\sin\theta_3+q_r\sin\theta_2\right]\right\}, \qquad (2)
\end{aligned}
$$

where k_1 is the side slope multiplied with flow depth to bottom width ratio, y_r is the flow depth ratio, B_r is the width ratio, F_1 is the Froude number, q_r is the discharge ratio, and $C=\frac{5}{6}-\frac{F_1^2}{40}-\frac{k_1}{12q_r}\left(\frac{1+2k_1}{(1+k_1)^2}\right)$ is constant in momentum transfer coefficient for trapezoidal channel junction.

Although the Froude number is more critical than Reynold's number, small turbulent fluctuations governed by Reynold's number may leads to unequal discharge distribution. In fact, the mathematical model of dividing flow that account for Reynold's number has never been discussed widely in literature. Therefore, this study proposes a new mathematical model aiming to accurately predict discharge distribution at the bifurcating or dividing channel. Since the angles in the channel junction affect the discharge of the channel after a junction, the relationship between the discharge ratio and division angles is also investigated.

2. Mathematical Formulations

This section provides a detailed description of the channel and formulation of the model. The dividing junction allows the water flow from main channel to be divided into two branch channels. The behavior of dividing flow is determined by applying the mass continuity and momentum principle with the following assumptions: the water flow is one dimensional and steady to the channel walls, velocity is uniformly distributed immediately above and below the junction, the wall friction is neglected as compared to other forces and the depth of the flow in main channel is equal to two branches.

The schematic layout and geometric details used for this study are shown in Figure 1. The water assumed to flow from the main channel (channel 1) to the branch channel (channel 2) and channel after junction (channel 3), where Q is the discharge in each channel, θ_2 and θ_3 are the division angles, b is the bottom width of the channel, a is side slope of the channel, β is angle of the slope slide, T is top width at the channel and y is depth of flow.

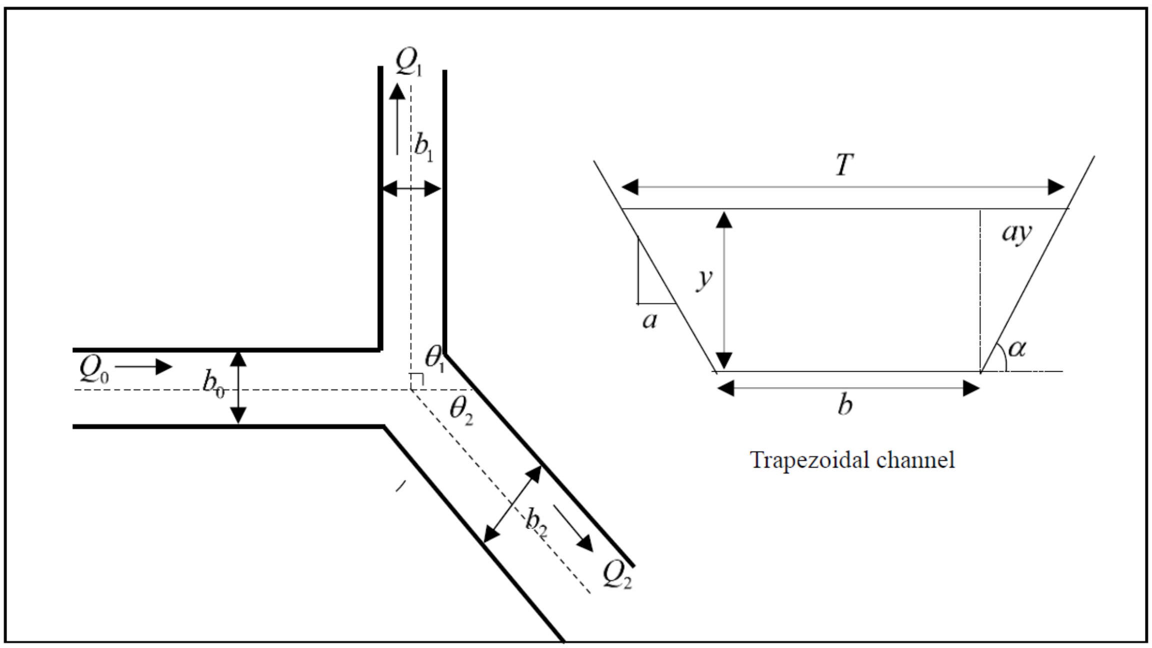

Figure 1: Schematic layout of open channel junction and trapezoidal channel

The following information are required to determine the geometric hydraulic properties (GHP) and solve the dividing flow equations which are hydraulic radius, $R_h = \dfrac{A}{P_w}$, where A is area and P_w is the wetted perimeter. The hydraulic depth is $D_h = \dfrac{A}{T}$, where T is top width of channel. The Manning's equation is the empirical approach that has been widely used to find the roughness coefficient, n in open-channel. Parsaie *et al.* (2017) investigated the discharge of the rivers by using Manning formula that possesses the values of roughness coefficients for natural channel (Teixeira *et al.* 2018). The roughness coefficient in the Manning velocity equation is one of the important parameters in the hydraulics of open channel, which can be determined based on field observations or the engineering judgements. A prismatic channel (trapezoidal cross-sectional channel) is chosen due to its constant bottom slope.

Manning's equation, $V = \frac{1}{n} R_h^{2/3} S^{1/2}$, where V is the velocity, n is the roughness coefficient and S is the average slope of channel. According to Nohani (2019), the Manning's roughness coefficient for the major river which came from Cowan method is $n = 0.035$. The velocity used in Froude number and Reynold's number of the equation is $V = 0.8571428571$. Froude number, $F_1 = \frac{V}{\sqrt{gD_h}}$ where $g = 9.80665\text{m/s}^2$ is gravity. The Froude numbers for each of the cross-sectional channels are different due to the different of hydraulic depth, yet the velocity and gravity are similar for different shapes.

Reynolds number, $\text{Re}_1 = \frac{VR_h}{\upsilon}$ considers viscosity of water, where $\upsilon = 1.004,$ is a kinematic viscosity, $\upsilon = \frac{\mu}{\rho}$. The density is $\rho = \frac{\gamma}{g}$ where $\gamma = 9.787114841$ is a specific weight of water and $\mu = 1.002$ is a dynamic viscosity. The kinematic viscosity, dynamic viscosity and specific weight of water have a certain value at a certain temperature (Kestin *et al.* 1978; Korson *et al.* 1969). The viscosity of any fluid type has a specific value at a particular temperature. In this study, the Reynolds number is considered as a parameter, while keeping the temperature constant at $20°$ Celsius in both the upstream and downstream sections of the channel.

Area of main channel, A_1 and branch channel, A_2 are assumed to be 1000m^2, while channel 3, A_3 is 200m^2. The flow depth for all branches is $y = 3.5\text{m}$. Various angles below $90°$ are considered to investigate its effect upon discharge ratio. A uniform flow is preferred to maintain the flow stability. The following information is required to derive the equation and find the geometric and hydraulic properties:

1. Area, $A = by + ay^2$.
2. Wetted perimeter, $P_w = b + 2\lambda$, where $\lambda = \sqrt{y + (ay)^2}$.
3. Top width, $T = b + 2ay$.
4. Angle of the slope side, β.

2.1 ***Mathematical model for trapezoidal channel***

In application of fluid dynamics, the momentum is known as the product of mass discharge and velocity. The general equation of momentum principle, which describes the conservation of momentum is given as follows:

$$-\rho QV_1 + \rho QV_2 = \overline{P_1}A_1 - \overline{P_2}A_2. \tag{3}$$

The general continuity equation, which describes the conservation of mass in open-channel as

$$Q = VA, \tag{4}$$

where
$\rho =$ fluid density
$Q =$ discharge
$V =$ flow velocity
$\overline{P} =$ average pressure
$A =$ the cross-sectional area of flow

The continuity equation, which states that the discharge must be conserved along the channel, is taken as starting point for the formulation,

$$Q_1 = Q_2 + Q_3, \tag{5}$$

where $Q_1 = A_1V_1$, $Q_2 = A_2V_2$ and $Q_3 = A_3V_3$. The terms Q_1, Q_2 and Q_3 are discharges, A_1, A_2 and A_3 are trapezoidal cross-sectional areas while V_1, V_2 and V_3 are velocities in the main channel, channel 2 and channel 3 respectively. The governing equation based on the momentum principle and continuity equation is

$$P_1 - P_3 \cos\theta_3 - P_2 \cos\theta_2 - U_3 - U_2 - \Delta P = \frac{\gamma}{g}(Q_3V_3 \cos\theta_3 + Q_2V_2 \cos\theta_2 - Q_1V_1). \tag{6}$$

The terms of momentum transfer are given as

$$U_2 = \rho Q_2 V_1 C \sin\theta_2, \tag{7}$$
$$U_3 = \rho Q_3 V_1 C \sin\theta_3. \tag{8}$$

This hydrostatic force is integrated from the interval 0 to y since the force is acting on a vertical channel.

$$P = \gamma A = \gamma \int_0^y by + ay^2 dA = \gamma \left[\frac{by^2}{2} + \frac{ay^3}{3} \right]_0^y = \gamma \left(\frac{by^2}{2} + \frac{ay^3}{3} \right). \tag{9}$$

Substitute Eq. (7) and Eq. (8) into Eq. (6),

$$\begin{aligned} &P_1 - P_3 \cos\theta_3 - P_2 \cos\theta_2 - \Delta P \\ &= \frac{\gamma}{g}(Q_3V_3 \cos\theta_3 + Q_2V_2 \cos\theta_2 - Q_1V_1 + Q_3V_1C \sin\theta_3 + Q_2V_1C \sin\theta_2), \end{aligned} \tag{10}$$

From the left-hand side of Eq. (10), the following expression is obtained:

$$P_1 - P_3 \cos\theta_3 - P_2 \cos\theta_2 - \Delta P, \tag{11}$$

where

$$\Delta P = \gamma\left(\frac{b_1 y_3^2}{2} + \frac{a y_3^3}{3}\right) - P_3 \cos\theta_3 .$$

Substitute Eq. (9) into Eq. (11)

$$\gamma\left[\left(\frac{b_1 y_1^2}{2} + \frac{a y_1^3}{3}\right) - \left(\frac{b_3 y_3^2}{2} + \frac{a y_3^3}{3}\right)\cos\theta_3 - \left(\frac{b_2 y_2^2}{2} + \frac{a y_2^3}{3}\right)\cos\theta_2 - \left(\frac{b_1 y_3^2}{2} + \frac{a y_3^3}{3}\right) + \left(\frac{b_3 y_3^2}{2} + \frac{a y_3^3}{3}\right)\cos\theta_3\right]. \tag{12}$$

Expand, simplify and factorise Eq. (12), yields

$$\gamma\left[\frac{1}{2}\left(b_1 y_1^2 - b_1 y_3^2 - b_2 y_2^2 \cos\theta_2\right) + \frac{a}{3}\left(y_1^3 - y_3^3 - y_2^3 \cos\theta_2\right)\right]. \tag{13}$$

From the right-hand side of Eq. (10),

$$\frac{\gamma}{g}(Q_3 V_3 \cos\theta_3 + Q_2 V_2 \cos\theta_2 - Q_1 V_1 + Q_3 V_1 C \sin\theta_3 + Q_2 V_1 C \sin\theta_2). \tag{14}$$

Expression Eq. (14) turns into

$$\frac{\gamma}{g}\left(\frac{Q_3 Q_3}{A_3}\cos\theta_3 + \frac{Q_2 Q_2}{A_2}\cos\theta_2 - \frac{Q_1 Q_1}{A_1} + \frac{Q_3 Q_1}{A_1} C \sin\theta_3 + \frac{Q_2 Q_1}{A_1} C \sin\theta_2\right). \tag{15}$$

Factorise Eq. (15) to produce

$$\frac{\gamma}{g}\frac{Q_1^2}{A_1}\left(\frac{Q_3^2 A_1}{A_3 Q_1^2}\cos\theta_3 + \frac{Q_2^2 A_1}{A_2 Q_1^2}\cos\theta_2 - 1 + \frac{Q_3}{Q_1} C \sin\theta_3 + \frac{Q_2}{Q_1} C \sin\theta_2\right). \tag{16}$$

By manipulating Eq. (16) algebraically,

$$\frac{\gamma}{g}\frac{Q_1^2}{A_1}\left[\frac{1}{Q_1^2}\frac{Q_3^2}{A_3/A_1}\cos\theta_3+\frac{1}{Q_1^2}\frac{Q_2^2}{A_2/A_1}\cos\theta_2-1+C\left(\frac{Q_3}{Q_1}\sin\theta_3+\frac{Q_2}{Q_1}\sin\theta_2\right)\right]. \tag{17}$$

To determine the discharge ratio, we assume $q_r=\frac{Q_2}{Q_1}$, where $Q_2=Q_1q_r$. From Eq. (5),

$$Q_1=Q_1q_r+Q_3. \tag{18}$$

Then Eq. (18) turns into $Q_3=Q_1-Q_1q_r$ and $Q_3=Q_1(1-q_r)$. Thus, $\frac{Q_3}{Q_1}=1-q_r$. Therefore, Eq. (17) becomes

$$\frac{\gamma}{g}\frac{Q_1^2}{A_1}\left\{\frac{(1-q_r)^2}{A_3/A_1}\cos\theta_3+\frac{q_r^2}{A_2/A_1}\cos\theta_2-1+C\left[(1-q_r)\sin\theta_3+q_r\sin\theta_2\right]\right\}. \tag{19}$$

The formula of Reynold's number, $\mathrm{Re}_1=\frac{V_1R_{h_1}}{\upsilon}$ can be expanded as

$$\mathrm{Re}_1=\frac{\frac{Q_1}{A_1}\frac{A_1}{P_{w_1}}}{\frac{\mu}{\rho}}=\frac{Q_1\rho}{P_{w_1}\mu}, \tag{20}$$

where $\rho=\frac{\gamma}{g}$. Rearrange Eq. (20),

$$P_{w_1}\mu\,\mathrm{Re}_1=Q_1\rho, \tag{21}$$

by squaring both sides of Eq. (21),

$$\frac{{P_{w_1}}^2\mu^2\,{\mathrm{Re}_1}^2}{\rho}={Q_1}^2\rho. \tag{22}$$

Multiply Eq. (22) both sides with $\frac{1}{A_1}$, yields

$$\frac{{P_{w_1}}^2\mu^2\,{\mathrm{Re}_1}^2}{\rho A_1}=\frac{{Q_1}^2\rho}{A_1}. \tag{23}$$

Hence, replace $\frac{\gamma}{g}\frac{Q_1^2}{A_1}$ in Eq. (19) by Eq. (23) to produce

$$\frac{P_{w_1}{}^2\mu^2 \mathrm{Re}_1{}^2}{\rho A_1}\left(\frac{(1-q_r)^2}{A_3/A_1}\cos\theta_3+\frac{q_r^2}{A_2/A_1}\cos\theta_2-1+C\left((1-q_r)\sin\theta_3+q_r\sin\theta_2\right)\right). \tag{24}$$

From Eq. (24), the coefficient C is derived by incorporating the Reynolds number into the formulation in Eq. (2), yielding

$$C=\frac{5}{6}-\frac{\left(\frac{\mathrm{Re}_1\,\mu}{\rho R_h}\right)^2}{40g\left(\frac{A_1}{T}\right)}-\frac{ay_1}{12b_1q_r}\left(\frac{b_1+2ay_1}{b_1+2ay_1+\frac{a^2y_1{}^2}{b_1}}\right), \tag{25}$$

Simplify Eq (25) and replace $R_h=\frac{A_1}{P_w}$ and $\rho=\frac{\gamma}{g}$ in Eq. (26), will become

$$C=\frac{5}{6}-\frac{\mathrm{Re}_1{}^2\,\mu^2T}{40gA_1\left(\frac{A_1}{P_w}\right)^2\left(\frac{\gamma}{g}\right)^2}-\frac{ay_1}{12b_1q_r}\left(\frac{b_1+2ay_1}{b_1+2ay_1+\frac{a^2y_1{}^2}{b_1}}\right). \tag{26}$$

Upon simplifying Eq. (26) and equating Eq. (13) with Eq. (24), the final model of dividing flow is obtained as follows:

$$\frac{\gamma^2A_1}{g}\left\{\frac{1}{2}\left(b_1y_1^2-b_1y_3^2-b_2y_2^2\cos\theta_2\right)+\frac{a}{3}\left(y_1^3-y_3^3-y_2^3\cos\theta_2\right)\right\}=$$
$$P_{w_1}{}^2\mu^2\mathrm{Re}_1{}^2\left\{A_1\left(\frac{(1-q_r)^2}{A_3}\cos\theta_3+\frac{q_r^2}{A_2}\cos\theta_2\right)-1+C\left[(1-q_r)\sin\theta_3+q_r\sin\theta_2\right]\right\}, \tag{27}$$

where $C=\frac{5}{6}-\frac{\mathrm{Re}_1{}^2\,\mu^2TgP_w{}^2}{40gA_1^3\gamma^2}-\frac{ay_1}{12b_1q_r}\left(\frac{b_1+2ay_1}{b_1+2ay_1+\frac{a^2y_1{}^2}{b_1}}\right).$

Since the velocity for both types of the equation are similar, the velocity from the Manning equation requires the value of the main channel slope to determine Reynold's number. By assuming the slope for channel 1 is $S_1 = 0.0001814260235$, the Reynold's number in the main channel becomes $\mathrm{Re}_1 = 2.837766734$, which represents the laminar flow. Eq. (27) is solved using Maple software to evaluate the discharge ratio, q_r at different bifurcation angles.

2.2 *The geometric and hydraulic properties*

The features of the channel such as flow depth, bifurcation angles, Reynold's number and bottom width of channel are important variables for the discharge computation. Table 1 presents the geometric and hydraulic properties (GHP) that are provided by Zawawi *et al.* (2019) to determine the discharge ratio.

Table 1. Geometric and hydraulic properties for trapezoidal cross-sectional channel

GHP	Main channel	Channel 2 (m)	Channel 3 (m)
α	60°	60°	60°
z	4.081632657m	4.081632657m	0.859291084m
T	300m	300m	60.15037594m
b	271.285714m	271.285714m	54.13533835m
λ	14.70821651m	14.70821651m	4.614668923m
P_w	300.8450044m	300.8450044m	63.3646762m
R_h	3.323970767m	3.323970767m	3.156332708m
D_h	3.33m	3.33m	3.325m

2.3 *Setting of* FLOW-*3D simulation*

The physical experiment in a hydraulic laboratory or computer simulation for results validation may not be accessible due to high cost and time-consuming. However, the validity of the proposed model in computing the discharge ratio at various bifurcation angles can be validated using a computational fluid dynamics (CFD) simulation software, that uses the Navier–Stokes equations and the volume of fluid (VOF) method to simulate and analyse complex fluid-based problem and interactions (Ghamam *et al.* 2023). FLOW-3D is widely used to validate the experimental results since it is known for its robustness and tendency to numerically reproduce flow with a clear visualisation power accurately (Sa'id Abdurrasheed *et al*. 2019). This software has advanced capabilities in modeling free-surface flows, such as in hydraulic engineering. FLOW-3D gained accuracy with percentage errors of less than 5% when compared with the experimental values. Therefore, in this study, the FLOW-3D simulation was conducted to validate the performance of the proposed mathematical model.

2.4 *Physics and fluid properties of FLOW-3D*

There are many physics options available in FLOW-3D, but only two selections are required. First is the gravity option with gravitational acceleration in the vertical (z) direction set to -9.81 m/s^2.

Second is the viscosity and turbulence model, where for this study, the Renormalised Group model was used, and the wall shear boundary condition is automatically set to a no-slip condition when the viscous flow is selected. In this setup, the fluid properties were based on the selected fluid. In this study, the temperature of water at 20° Celsius was used. The density and viscosity of water are 1000 kg/m^3 and 0.001 kg/m/s, respectively. Other parameters remained constant as default.

2.5 *Meshing and geometry*

The preparation of model geometry is different for each simulation. For a bifurcated channel, the geometry was drawn in AutoCAD and exported in stereolithographic (stl) format. The most crucial part in CFD simulation is to determine an appropriate meshing size. The mesh and cell size can affect the accuracy and simulation time. In this study, the relative proportions of the computational domain dimensions are determined by the size ratio is (2: 2: 1) for each (x (length): y (width): z (height)), which does not exceed maximum size ratio 3:1 between two directions. After a suitable mesh is selected, the FAVORized tool is used to visualise the geometry so that it is sufficiently realistic with enough resolution to capture important features of the flow. Figures 2 and 3 show the actual and FAVORized geometry of the channel, respectively. The roughness property of the geometry is set to 0.242, equivalent to 0.03 manning's coefficient, n. The purpose of flux surface, which is located in each channel is to measure discharge and velocity in main and branch channels.

Figure 2: Actual geometry of the channel

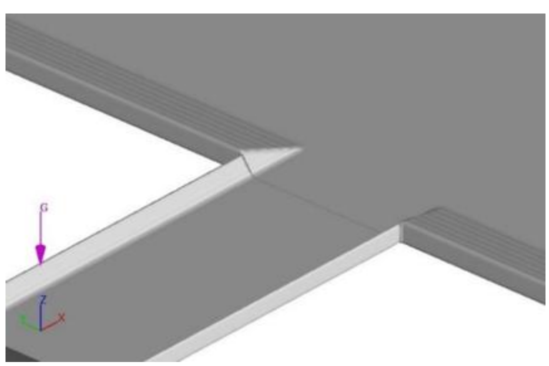

Figure 3: FAVORized geometry of the channel

2.6 *Boundary and initial conditions*

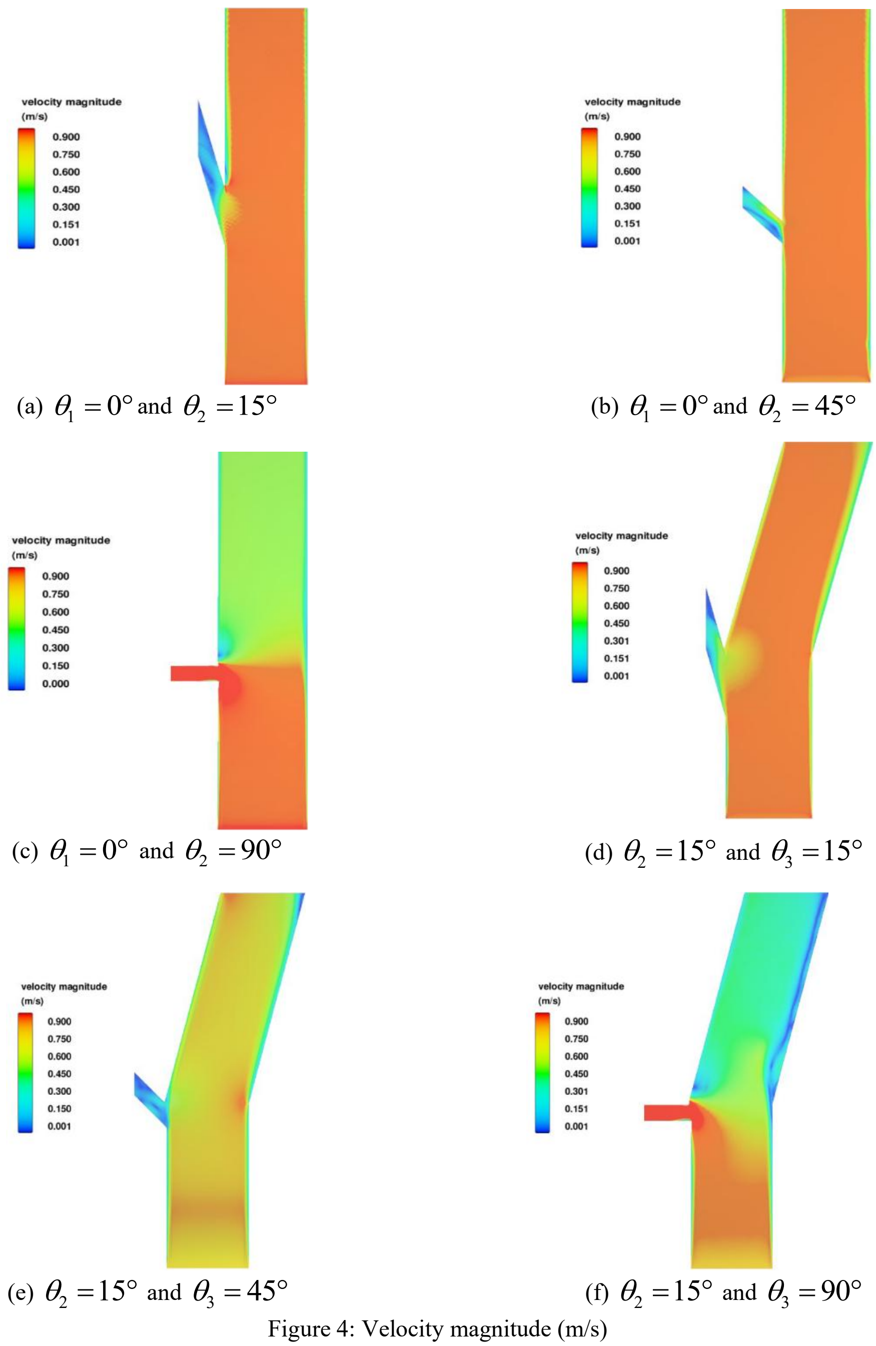

(a) $\theta_1 = 0°$ and $\theta_2 = 15°$ (b) $\theta_1 = 0°$ and $\theta_2 = 45°$

(c) $\theta_1 = 0°$ and $\theta_2 = 90°$ (d) $\theta_2 = 15°$ and $\theta_3 = 15°$

(e) $\theta_2 = 15°$ and $\theta_3 = 45°$ (f) $\theta_2 = 15°$ and $\theta_3 = 90°$

Figure 4: Velocity magnitude (m/s)

Boundary conditions define how fluid interacts with the edges of the computational domain. This condition is originally set to symmetry (S), which means no flow or heat transfer across this boundary. To study the discharge in the main and branch channels, the boundary condition at the main channel upstream is set to volumetric discharge (Q) and outflow (O) boundary conditions for both branch channels. The boundary at the top of the channel is set to a pressure (P) boundary condition, while the boundary at the bottom channel remains as default.

Initial conditions define the starting state of the fluid in the domain before the simulation begins. It follows the actual flow data of the water elevation and hydrostatic pressure. The discharge at the upstream is gradually increased from zero to the required discharge to reduce water splashing and immediate change of velocity, hence increasing the stability of the simulation and shortening the time to reach its steady state. The setting of boundary and initial conditions will affect the simulation results as shown in Figures 4.

3. Results Analysis

This section discusses the results of the mathematical models and numerical simulation. It has to be mentioned that the angles used in channel 3, θ_3 are $0°, 15°, 30°, 45°, 60°, 75°$ and $90°$, while the simulation results as shown in the previous section are available only for the case of the trapezoidal channel with $\theta_2 = 0°$ and $\theta_2 = 15°$. Tables 2 and 3 show the discharge ratio for each model and its deviation percentage for the open-channel dividing flow with Reynold's in trapezoidal channel model (OCDFR-T), previous model of open-channel dividing flow in trapezoidal channel (OCDF-T) provided by Zawawi *et al.* (2019) (Eq. (2)) and FLOW-3D simulation. The deviation percentage for OCDFR-T and OCDF-T is determined as follows:

$$\text{Deviation percentage (\%)} = \left| \frac{q_r^{Model} - q_r^{FLOW3D}}{q_r^{FLOW3D}} \right| \times 100,$$

where q_r^{Model} is the discharge ratio of the OCDFR-T or OCDF-T, while q_r^{FLOW3D} is the discharge ratio of the FLOW-3D simulation.

Table 2. The discharge ratio, q_r when $\theta_2 = 0°$

θ_3	OCDFR-T (Proposed model)	OCDF-T (Zawawi *et al.* 2019)	FLOW-3D	Deviation Percentage (%)	
				OCDFR-T	OCDF-T
15°	0.8468182695	0.8226499373	0.9815875219	13.73	16.19
30°	0.8511742960	0.8283690369	0.9785935509	13.02	15.35
45°	0.8439906764	0.8213714460	0.9766275734	13.58	15.90
60°	0.8166283420	0.7927880538	0.9502719692	14.06	16.57
75°	0.7382896595	0.7125397288	0.8518835633	13.33	16.36
90°	0.4138210173	0.4162893823	0.5132984892	19.38	18.90

From Table 2, the results show that the OCDFR-T model consistently exhibits lower deviation values compared to the OCDF-T model for all division angles except for $\theta_3 = 90°$. However, at

$\theta_3 = 90°$ (perpendicular branch or T-junction), the OCDFR-T and OCDF-T model show the same deviation percentage (18.90%). This consistency underscores the improved predictive alignment of OCDFR-T with the FLOW-3D simulation. The smallest deviation for the proposed model occurs at $\theta_3 = 30°$ (13.00%), while the largest is observed at $\theta_3 = 90°$ (18.90%). The deviations in the OCDF-T remain uniformly higher when ranging from 15.35% to 18.90%.

Table 3. The discharge ratio, q_r when $\theta_2 = 15°$

θ_3	OCDFR-T (Proposed model)	OCDF-T (Zawawi *et al*. 2019)	FLOW-3D	Deviation Percentage (%)	
				OCDFR-T	OCDF-T
15°	0.8333117284	0.8066937934	0.9300000000	10.40	13.26
30°	0.8364214752	0.8110025330	0.9600000000	12.87	15.52
45°	0.8265790842	0.8010032400	0.9800000000	15.66	18.26
60°	0.7937457131	0.7663336286	0.9400000000	15.56	18.48
75°	0.7020171223	0.6717354488	0.7600000000	7.63	11.61
90°	0.3175102713	0.3194043084	0.4300000000	26.16	26.72

Table 3 shows that the OCDFR-T consistently have a lower deviation value for all division angles compared to OCDF-T. The smallest deviation for the OCDFR-T is observed at $\theta_3 = 75°$ (7.53%), while the highest deviation is at $\theta_3 = 90°$ (25.72%). Both models exhibit a higher deviation when $\theta_3 = 90°$, which is due to the perpendicular branches or T-junction that create complex behavior including separation and velocity distribution. However, OCDFR-T remains comparably better result even in this division angle.

Figures 2 and 3 show the graphs of discharge ratio, q_r against division angles, θ_3 when $\theta_2 = 0°$ and 15° for trapezoidal channel. A similar trend of discharge ratio occur between OCDFR-T, OCDF-T and FLOW-3D, where all discharge values is lower than the critical value of 0.8. It is observed that $\theta_3 = 90°$ can be paired with $\theta_2 = 0°$ or 15° to prevent the overflow in the channel 3. Both Figures 5 and 6 show a similar trend of discharge ratio, where an increase in the division angle in channel 2 results in a slight increase in the discharge ratio, followed by a sudden decrease for angles greater than 45°. Furthermore, the discharge ratio obtained by proposed model is closer to the FLOW-3D simulation compared to the model proposed by Zawawi *et al.* (2019). This closer agreement is attributed to the Reynolds number accounting for viscous effects, which significantly influence the discharge ratio in dividing channels.

The difference between the results of simulation and mathematical modelling is most probably due to inaccurate boundary conditions used in simulation or assumptions made. For example, a mathematical model may assume that the flow is steady-state, whereas in reality, the flow may be unsteady. Meanwhile, the viscosity of the fluid may vary with temperature, which the mathematical model may not account for. In contrast, FLOW-3D simulation solves the full Navier-Stokes equations in three-dimension, allowing for the detailed modelling of free-surface flow, turbulence and realistic channel geometries.

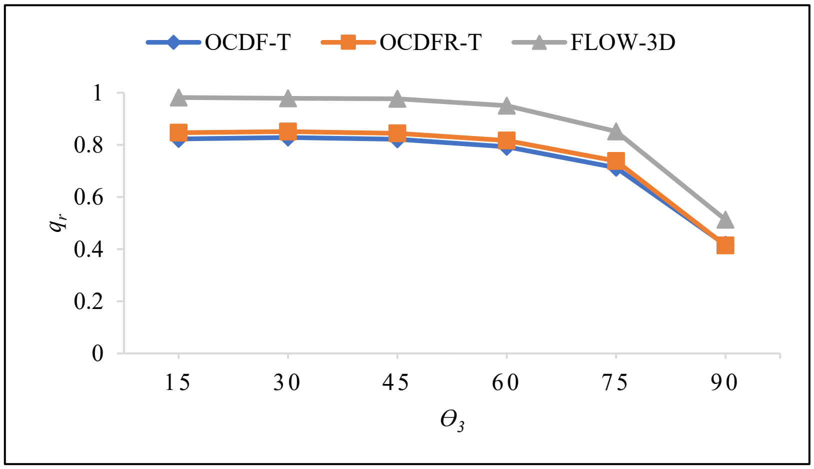

Figure 5: Graph of the discharge ratio, q_r against bifurcation angles, θ_3 when $\theta_2 = 0°$ for trapezoidal channel

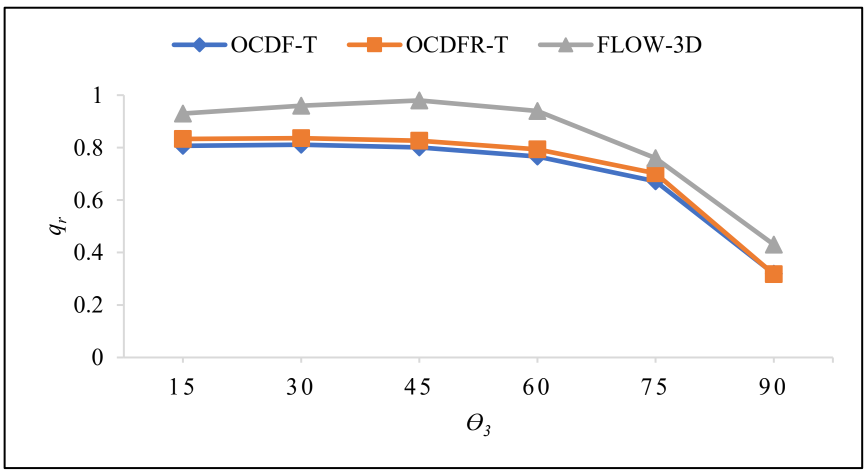

Figure 6: Graph of the discharge ratio, q_r against bifurcation angles, θ_3 when $\theta_2 = 15°$ for trapezoidal channel

4. Conclusion

In this study, a new mathematical model of dividing open-channel flow with trapezoidal cross-sectional channel has been derived based on the Reynold's number in the main channel to investigate the relationship between discharge ratio and bifurcation angles. In the context of an open channel flow, Reynold's number is an important parameter because it determines whether the flow is laminar or turbulent, which affects the shear stresses and frictional losses in the channels. The discharge in an open channel dividing flow that is influenced by the Reynolds number affects the mixing and momentum transfer between the channels. However, the exact relationship between these parameters and the discharge depends on the GHP, Manning's roughness, as well as the properties of the fluid itself. By incorporating the Reynold's number in a mathematical model, the model can more accurately simulate the behavior of the discharge, particularly at locations where flow separation or other complex flow phenomena occur. This can result in more accurate predictions and better decision-making. The use of these parameters may improve the efficiency of the modelling process, as it allows for the simplification of the model while maintaining accuracy. This can save time and resources and make the modelling process more accessible to researchers and engineers.

Both simulation software and mathematical models can be useful tools for estimating discharge ratios in open channel flow systems. FLOW-3D can provide a more detailed and accurate representation of the flow behavior, including complex phenomena, but may require more computational resources and expertise to use effectively. Meanwhile, mathematical models, on the other hand, can provide simpler and faster solutions, but may not capture all the details of the flow behavior. The choice between using both methods for estimating discharge ratios depends on the specific requirements of the research and available resources. In some cases, a combination of both approaches may be used, with simulation software providing more detailed information about the flow behavior in specific regions, while mathematical models provide simpler and computationally efficient solutions for the overall system. The Department of Irrigation and Drainage can utilise this analysis to execute the bifurcation of the river in the flood-prone area, since it provides optimal angles for separating the river to alleviate floods.

Acknowledgments

The research was supported by Universiti Teknologi MARA (UiTM), Shah Alam, Selangor, Malaysia. This research was conducted in collaboration with Universiti Teknologi Malaysia (UTM).

Nomenclatures

A : Cross-sectional area of the channel
C : Constant
F : Froude number
g : Gravitational acceleration
k : Side slope x flow depth to bottom width ratio
P : Pressure force
W_p : Wetted perimeter
Q : Discharge
q_r : Discharge ratio
b : Bottom width of the channel
B_r : Width ratio
T : Top width of the channel
U : Momentum transfer
V : Flow velocity

y : Flow depth

y_r : Flow depth ratio

ρ : Specific gravity

γ : Specific weight

θ : The angle of the dividing channel

References

Abu-Zaid T.S. 2023. Three-dimensional numerical study for determining the optimum diversion angle of bifurcating channels. *Ain Shams Engineering Journal* **14**(4): 101940.

Ahammed N., Asirvatham L.G. & Wongwises S. 2016. Effect of volume concentration and temperature on viscosity and surface tension of graphene–water nanofluid for heat transfer applications. *Journal of Thermal Analysis and Calorimetry* **123**(2): 1399–1409.

Alfatlawi T.J.M. & Hussein A.H. 2024. A numerical study of diversion flow to determine the optimum flow system in open channels. *Water Practice & Technology* **19**(4): 1330–1347.

Alomari N.K., Yusuf B. & Mohammad T.A. 2016. Flow in a branching open channel: a review. *Pertanika Journal of Scholarly Research Reviews* **2**(2): 40–56.

Alomari N.K., Yusuf B., Mohammad T.A. & Ghazali A.H. 2020. Influence of diversion angle on water and sediment flow into diversion channel. *International Journal of Sediment Research* **35**(6): 600–608.

Azimi H. & Shabanlou S. 2016. Comparison of subcritical and supercritical flow patterns within triangular channels along the side weir. *International Journal of Nonlinear Sciences and Numerical Simulation* **17**(7–8): 361–368.

Cao J., Kraut M., Dittmeyer R., Zhang L. & Xu H. 2018. Numerical analysis on the effect of bifurcation angle and inlet velocity on the distribution uniformity performance of consecutive bifurcating fluid flow distributors. *International Communications in Heat and Mass Transfer* **93**: 60–65.

Cheng T., Wang J. & Sui J. 2018. Calculation of critical flow depth using method of algebraic inequality. *Journal of Hydrology and Hydromechanics* **66**(3): 316–322.

Esfe M.H., Afrand M., Gharehkhani S., Rostamian H., Toghraie D. & Dahari M. 2016. An experimental study on viscosity of alumina-engine oil: effects of temperature and nanoparticles concentration. *International Communications in Heat and Mass Transfer* **76**: 202–208.

Ghamam A.S., Abohatem M.A., Mohd Haniffah M.R. & Othman I.K. 2023. The Relationship Between Flow and Pressure Head of Partially Submerged Orifice Through CFD Modelling Using Flow-3D. *Proceedings of the 5th International Conference on Water Resources (ICWR) – Volume 1. Lecture Notes in Civil Engineering*, pp. 235–250. Springer: Singapore.

Harmizi P.N.S. & Zawawi I.S.M. 2024. Mathematical modeling of the flow division in V-shaped cross-sectional channel. *AIP Conference Proceedings*, p. 030010.

Ibrahim I., Legori Ibrahim S. & Khan S. 2020. Flow structures in dividing open channels: A review. *IOP Conference Series: Earth and Environmental Science*, pp. 12008.

Karimi S.M. 2018. *Modeling fluid flow in an open rectangular channel with lateral inflow channel*. Pan African University.

Kestin J., Sokolov M. & Wakeham W.A. 1978. Viscosity of Liquid Water in the range of -8 C and 150 C. *Journal of Physical and Chemical Reference Data* **7**(3): 941–948.

Kleinhans M.G., Ferguson R.I., Lane S.N. & Hardy R.J. 2013. Splitting rivers at their seams: bifurcations and avulsion. *Earth Surface Processes and Landforms* **38**(1): 47–61.

Korson L., Drost-Hansen W. & Millero F.J. 1969. Viscosity of water at various temperatures. *The Journal of Physical Chemistry* **73**(1): 34–39.

Liu H. & Li P. 2013. Even distribution/dividing of single-phase fluids by symmetric bifurcation of flow channels. *International Journal of Heat and Fluid Flow* **40**: 165–179.

Malik L. & Matin M.A. 2021. Experimental study on flow and sediment distribution at off-take channel. *International Journal of Environmental Science and Development* **12**(2): 35–41.

Nohani E. 2019. Estimating the Manning's Roughness Coefficient in Rivers by Experimental Method. *Foot* **1**(6): 5–7.

Pandey A.K. & Mishra R. 2012. Comparison of flow characteristics at rectangular and trapezoidal channel junctions. *Journal of Physics: Conference Series*, pp. 12141.

Parsaie A., Najafian S., Omid M.H. & Yonesi H. 2017. Stage discharge prediction in heterogeneous compound open channel roughness. *ISH Journal of Hydraulic Engineering* **23**(1): 49–56.

Sa'id Abdurrasheed A., Wan Yusof K., Hamid Hussein Alqadami E., Takaijudin H., Ab. Ghani A., Muhammad M.M., Sholagberu A.T., Zainalfikry M.K., Osman M. & Shihab Patel M. 2019. Modelling of Flow Parameters through Subsurface Drainage Modules for Application in BIOECODS. *Water* **11**(9): 1823.

Shahari N.A., Norwaza N.A.H., Zawawi I.S.M., Kamarul N.A.M. & Said A. 2021. Numerical investigation on the behavior of combining open-channel flow. *Indonesian Journal of Electrical Engineering and Computer Science* **23**(2): 1110–1119.

Teixeira E.K. da C., Coelho M.M.L.P., Pinto E.J. de A., Diniz J.G. & Saliba A.P.M. 2018. Manning's roughness coefficient for the Doce River. *Revista Brasileira de Recursos Hidricos* **23**: e52.

Toghraie D., Alempour S.M. & Afrand M. 2016. Experimental determination of viscosity of water based magnetite nanofluid for application in heating and cooling systems. *Journal of Magnetism and Magnetic Materials* **417**: 243–248.

Zawawi I.S.M., Abdullah N.L., Aris H., Jaafar B.A., Norwaza N.A.H. & Yunos M.H.F.M. 2019. Mathematical modeling for flood mitigation: Effect of bifurcation angles in river flowrates. *Civil Engineering and Architecture* **7**(6A): 50–57

Faculty of Computer and Mathematical Sciences
Universiti Teknologi MARA
40450 Shah Alam
Selangor, MALAYSIA
E-mail: iskandarshah@uitm.edu.my[*]*, puterinadiaharmizi@gmail.com*

Department of Water and Environment Engineering
School of Civil Engineering
Universiti Teknologi Malaysia
81310 Johor Bahru
Johor, MALAYSIA
E-mail: mridza@utm.my, saasyarah2@graduate.utm.my

Received: 10 November 2025
Accepted: 27 January 2026

*Corresponding author